Remote Sensing Applications: Society and Environment 23 (2021) 100563

Contents lists available at ScienceDirect

Remote Sensing Applications: Society and Environment

journal homepage: www.elsevier.com/locate/rsase

Addressing management practices of private forests by remote sensing and open data: A tentative procedure

E.J. Momo, S. De Petris, F. Sarvia *, E. Borgogno-Mondino

Department of Agricultural, Forest and Food Sciences, University of Turin, L.go Braccini 2, Grugliasco, 10095, Italy

ARTICLE INFO

Keywords:
Artificial neural network
Sentinel-2
Forest planning
NDVI
NDWI

ABSTRACT

The qualitative and quantitative knowledge of forestry stands is a fundamental requirement for their management and exploitation planning. Traditional field measurements, based on plots, are certainly accurate, but time-consuming and expensive; moreover, it cannot provide a wall-to-wall estimate of measures over large areas. Even though they are essential for calibrate and validate models and respectively results, remote sensing could be a useful support for forest planners when trying to describe wide areas. Optical images from medium-high resolution satellite missions are widely employed due to their accessibility, affordability and readiness to use. Within this framework, in this study an approach based on open-data from the Copernicus Sentinel-2 mission and Regional low density LiDAR data was developed in order to assess private forest wood resource in the Susa Valley (Piemonte Region, NW - Italy). The proposed methodology aims to support private forest management by the local forest consortium for basal area and wood volume estimation of forest stands. Specifically, the process was based on the jointly use of Multi-layer Perceptron (MLP) artificial neural network (ANN), trained and validated with respect to ground data from 285 surveyed plot. Furtherly, to refined wood volume estimates correcting factors accounting for slope and local stand fertility were applied. Estimates of volume stands were generated separately for conifers and broadleaves. Results prove that the adoption of correcting factors improved volume estimates by the MLP and ANN about 2% (relative mean absolute error) and 13% in conifer and broadleaf stands respectively.

1. Introduction

The qualitative and quantitative knowledge of forestry stands is a fundamental requirement for their management and planning. Tree height, diameter at breast height (DBH), basal area (BA) and volume (V) are essential parameters for foresters to assess current or prospective commercial value of forest stands and to plan thinning and cutting (Morin et al., 2018). Traditional field measurements, based on plots, are certainly accurate, but time-consuming and expensive (Chave et al., 2014) and cannot provide a continuous spatial description of data over wide areas (Vacchiano et al., 2018). As a consequence, they are suitable for a small area application only. Even though field measurement is absolutely essential for calibrating dendrometric/hypsometric models and assessing results (Galidaki et al., 2017), remote sensing could be a useful support for forest planners. In fact, biomass estimation by remote sensing, in addition to reduce the field work, offers continuous and consistent estimates at multiple scales (Fang et al., 2019).

Nevertheless, estimates of forest biomass based on remote sensing can generate inconsistent results mainly due to the lack of a direct relationship between spectral signal and biomass, especially in broad-leaved forests and for coppices stands, where the relationship between stem and foliage mass is inherently different than in high forests (Vacchiano et al., 2018). Moreover, the value of remote sensing data to estimate forest parameters such as DBH, AGB (above ground biomass), carbon stocks, tree height and density has been demonstrated (Morin et al., 2019). Many studies dealings with both climate change and sustainability of forest management based on remotely sensed data can be found in literature (Dube et al., 2016; Monserud 2003; Bravo et al., 2008).

Many of them propose different methods for the estimation of forest biomass-related features and a wide variety of approaches have been used relying on optical, LiDAR (Light Detection And Ranging) and radar data; they include parametric (e.g. regression models) and non-parametric approaches such as K-Nearest Neighbour (K-NN) and

* Corresponding author.
E-mail addresses: evelynjoan.momo@unito.it (E.J. Momo), samuele.depetris@unito.it (S. De Petris), filippo.sarvia@unito.it (F. Sarvia), enrico.borgogno@unito.it (E. Borgogno-Mondino).

https://doi.org/10.1016/j.rsase.2021.100563
Received 11 May 2021; Received in revised form 7 June 2021; Accepted 8 June 2021
Available online 11 June 2021

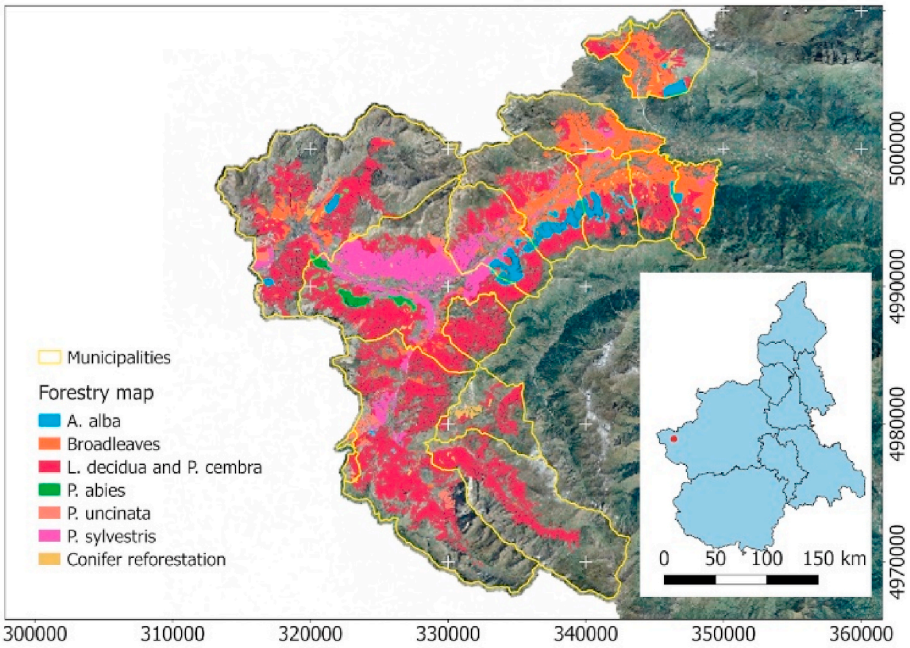

Fig. 1. Study area location and forest types. Reference system is WGS84 UTM 32N.

Random Forest estimator, Artificial Neural Network (ANN), Support Vector Machine (SVM), Maximum Entropy (MaxEnt, (Fassnacht et al., 2014; Lu et al., 2016). Non-parametric approaches, recently, have become more prevalent due to their higher potential to identify unknown complex nonlinear relationships (Haywood et al. 2018). Within this context, optical images from medium-high resolution satellite missions are widely employed due to their accessibility, affordability and readiness to use (Dube et al., 2016). The importance of the SWIR (short wave infrared), NIR (near infrared) and Red Edge bands for stand parameters estimation (e.g. AGB, BA and V) is well known from literature (Chrysafis et al., 2017). It was also observed that the green band is a good predictor for the BA and growing stock volume (Astola et al., 2019). In some studies, native spectral bands are used to calibrate empirical regression models for biomass estimation (Vacchiano et al., 2018; Zhao et al., 2016); in others, vegetation indices are used trying to better synthesize complex information (Freitas et al. 2005; Pandit et al. 2018). In other works, optical data were jointly used with LiDAR or radar ones (Jiménez et al., 2017; Morin et al., 2018; Wittke et al., 2019) or, alternatively, with reference to topographic parameters, such as altitude and slope (Gonçalves et al., 2019). Additionally, repeatability of satellite acquisitions permits multitemporal analysis of forests making possible to improve single acquisition deductions (Mura et al., 2018).

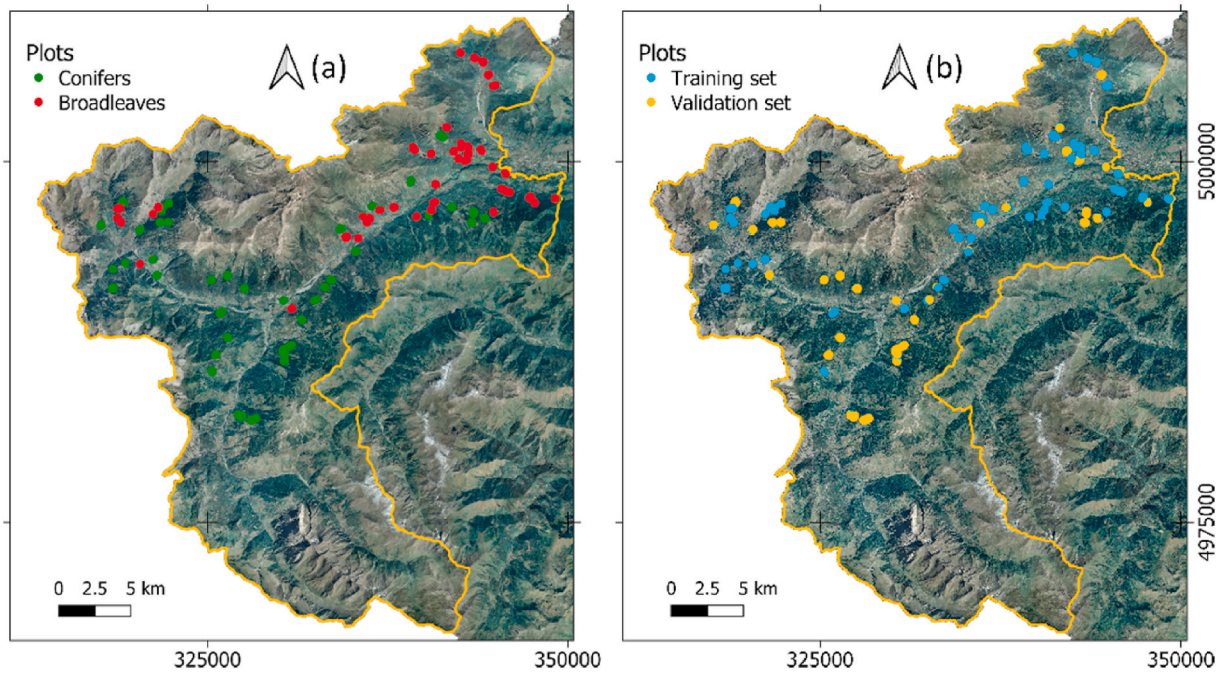

Fig. 2. (a) Ground-plots location within conifers and broadleaves stands; (b) Training and test sets location over the study area. Reference system is WGS84 UTM 32N.

Concerning accuracy of estimates, radar-based methods appear to be efficient on a large area analysis, but suitable for homogenous stands only (Dittmann, Thiessen, and Hartung, 2017); they also prove to saturate in forest characterized by a high level of biomass (Dube et al., 2016). Otherwise, LiDAR based approaches appear to be the most efficient and accurate ones for medium sized area applications. Differently, multispectral imagery appears to be appropriate for large area monitoring (Naik et al. 2021). Unfortunately, in general, satellite optical data generate a coarse estimation of homogeneous stands, and some further limitations can be observed in mountain regions (Dittmann, Thiessen, and Hartung, 2017).

Within these premises, in this study an approach based on open-data (multispectral satellite images and LiDAR data) was developed in order to assess private forest wood resource in Piemonte Region (NW- Italy). Ordinary, in Italy private forests are characterized by low economic value due to poor timber quality generated by no silvicultural management. Piemonte Regional Forestry Plan (NW Italy) recognizes a lack between wood harvesting cost and resulting timber low market value (Rizzo et al., 2019; Nocentini 2009). Within this economic issue, costs are expected to be possibly reduced if forest biomass estimation is supported by remote sensing; this would limit the ordinary workflow where required field surveys and difficulty in areas accessing determine high costs, mainly related to time consuming (Lu 2006). Therefore, authors present a possible methodology for the estimation of BA and V of private forest stands in the study area, with the aim of supporting their management by the High Susa Valley Forest Consortium (hereinafter called CFAVS). Methodology relies on freely available satellite imagery from the Copernicus Sentinel-2 mission and Regional low density LiDAR data; processing is based on Multi-layer Perceptron - MLP (Rumelhart et al. 1985), artificial neural network (ANN) trained and validated with respect to ground data from 285 surveyed plots.

2. Material and methods

2.1. Study area

The study area is located in Susa Valley (Italian North-Western Alps), within the territory managed by the CFAVS including the municipalities of Bardonecchia, Cesana Torinese, Claviere, Exilles, Oulx, Salbertrand, Sauze di Cesana, Sauze d'Oulx, Chiomonte, Gravere and Giaglione (NW Italian Alps - Fig. 1). The study area sizes about 69,150 ha and altitude ranges between 600 and 3200 m above mean sea level; climate is continental (Peel et al., 2007). According to the available regional forest types map (Camerano et al., 2017), forested areas cover about 30,973 ha, the 30% are private forests, with a prevalence of conifers 79% of the total forested area (mainly: larch, scot pine, silver fir). The remain 21% are broadleaves (mainly chestnut, beech and associations of maple, ash and linden).

2.2. Available data

2.2.1. Ground data

In order to calibrate and validate the proposed method, 285 circular plots (radius = 15 m) were surveyed; 148 out of them were dominated by conifers, 137 by broadleaves (Fig. 2a). For each plot all trees having diameters greater than 7.5 cm were considered and DBH, BA and V were collected. The latter was estimated adopting the local double-entry tree volume table of the CFAVS for *Abies alba* (Mill.) (silver fir), *Picea abies* (L.) (European spruce), *Larix decidua* (Mill.) (European larch) and *Pinus cembra* (L.) (Stone pine) and the double-entry tree volume table for the *Fagus sylvatica* (L.) (European beech) (Nosenzo 2008). For the other species the equations of the Carbon National Forest Inventory (INFC2005) were applied. Plot position was georeferenced in respect of their central point that was surveyed by Trimble GeoExplorer GNSS (Global Navigation Satellite System) receiver having an accuracy of about 0.7 m after differential correction of C/A code measures recorded with a time step of 5 s for more than 10 min. Finally, the 80% of the plots was randomly selected constituting the training set that was used to train ANN, while the 20% was used to test the basal area and volume maps (Fig. 2b). All plots were located in private stands and were equally distributed in respect of the main forest classes to ensure a similar representativeness during procedure calibration and ANN training.

Table 1
S2 images (Level-2A) used for this work. The study area is located between two S2 tiles (T32TLQ and T32TLR) aligned along the same orbital path (timely coherent).

ID	Date
1	June 19, 2018
2	July 29, 2018
3	August 28, 2018
4	September 27, 2018

2.2.2. Sentinel-2 imagery

Four Sentinel 2 (S2) level-2A images were obtained from the Open Data Hub of the EU Copernicus program. Level-2A data were provided already orthoprojected into WGS84 UTM32N reference frame and calibrated at-the-ground-reflectance. One image per month was obtained along the growing season concerning the period June–September 2018 (Table 1) in order to take care about temporal spectral variability and improve BA estimation as highlighted by (Shang et al., 2019). Selected images were those presenting the minimum cloud cover in the considered month. Sentinel 2 imagery has a spectral resolution of 13 bands having different geometric resolution (GSD, Ground Sampling Distance). In this work only the green (560 nm), red (665 nm), NIR (842 nm) and SWIR1 (1650 nm) bands were selected in order to compute some spectral indices useful to assess forest biomass status/density. The previous-mentioned bands have a nominal GSD equal to 10 m for green, red, NIR bands; 20 m for medium infrared one.

2.2.3. Lidar-derived data

To refine ANN estimates a low-density LiDAR dataset (L) obtained from the Piemonte Region Cartographic Office was also used (http://www.geoportale.piemonte.it). L dataset was acquired during the so-called ICE aerial-photogrammetric survey (2009–2011) by LEICA ALS50-II sensor (Leica Geosystems, 2006). Region Cartographic Office provided also the digital terrain model (DTM) and digital surface model (DSM) derived by a L processing. In particular, filtered LiDAR returns were classified into "ground" and "not-ground" and were regularized and provided by regional geoportal into DTM and DSM having nominal GSD equal to 5 m. DSM height accuracy was 0.72 m as reported by (Borgogno Mondino et al., 2016).

2.3. Data processing

2.3.1. Dendrometric models calibration

V and BA are silvicultural parameters used to measure the amount of wood existing in a forestry stand. Nevertheless, BA proved to be more strongly correlated with the spectral properties of canopy, since it only depending on tree diameter that it is directly related to the size of the canopy itself (Reis et al., 2018). For this reason, it was decided to focus on BA in place of V as forest parameter possibly estimable by remotely sensed data. V was derived in a second step from the estimated BA adopting self-calibrated dendrometric models. The regression between BA and V was tested with respect to available ground measures and the relationship modelled by a 1st order polynomial (eq. (1)), making possible to translate the map of estimate of BA into the correspondent map of V.

$$V = a \cdot BA + b \quad (1)$$

Table 2
Spectral Indices formulae adopted where ρGREEN, ρRED, ρNIR, ρSWIR1 are the reflectance at 560 nm, 665 nm, 842 nm and 1650 nm respectively.

Spectral Index	Formula	Reference
Normalized Difference Vegetation Index (NDVI)	$NDVI = (\rho_{NIR}-\rho_{RED})/(\rho_{NIR}+\rho_{RED})$	Rouse et al. (1974)
Normalized Difference Water Index (NDWI)	$NDWI=(\rho_{GREEN}-\rho_{SWIR1})/(\rho_{GREEN}+\rho_{SWIR1})$	Xu (2006)

Where V is the wood volume ($m^3 \cdot ha^{-1}$) according to ground data, BA is the BA ($m^2 \cdot ha^{-1}$) according to ground data and a, b are the regression parameters estimated using ordinary least squares method. Two separate dendrometric models were calibrated considering BA and V of conifers and broadleaves.

2.4. Vegetation indices computation

Starting from S2 selected bands, two spectral indices were computed for each image in the considered period, in particular the normalized difference vegetation index (NDVI) and normalized difference water index (NDWI) were selected and reported in Table 2. Final vegetation index maps were generated and called: NDVI1, NDWI1, NDVI2, NDWI2, NDVI3, NDWI3, NDVI4 and NDWI4 where 1, 2, 3, 4 are the month acquisition i.e. June, July, August and September respectively. These indices, in fact, proved to be correlated to forest stands density and biomass (Barbachea et al. 2018). Mean index value was computed for each surveyed plot in the training set by ordinary zonal statistics tools performed in SAGA GIS 7.0 software (Conrad et al., 2015). These data were used as inputs to design and train the MLP ANN dedicated to BA estimation.

2.4.1. ANN-retrieved basal area

In order to produce the final map of estimated BA geometrically consistent with the size of the plots, all vegetation index map were downsampled from 10 to 40 m by average method. All downsampled maps of indices were finally stacked in a single file to feed the trained ANN and obtaining a map of BA estimate in every forested pixel of the valley. With reference to the 4 downsampled images, the correspondent 4 NDVI and 4 NDWI maps were used as predictors (total layers adopted was 8) of BA within a MLP ANN. ANN training set and test set were obtained coupling the above-mentioned averaged measures of NDVI/NDWI within the surveyed plots (inputs) with the correspondent BA values computed, for the same plots, from ground measures. Conifers and broadleaves plots were processed separately and two different ANNs trained.

To find a configuration matching a reasonable accuracy of estimates, a self-developed routine was implemented in MATLAB R2018b (Borgogno Mondino, Giardino, and Perotti 2009; Lessio, Mondino, and Alma 2011) based on the Neural Network Toolbox. The routine is in charge of testing iteratively different ANN configurations by varying selectively the number of neurons in the hidden layer; for each architecture the seed for weights initialization is changed for a number of times depending on user (one of the routine parameters). It stops when an appropriate accuracy level for the estimates of the BA is found. When both of them are found to be lower than the reference thresholds (the user has to set them up) ANN is assumed as properly trained and, consequently, used to generate estimates of BA in the whole area. During iterations, the number of inputs is maintained fixed. ANN training algorithm is an ordinary back-propagation one, based on the Levenberg-Marquardt approach. Accuracy test is operated with respect to relative mean absolute error of training set ($rMAE_{TR}$) and relative mean absolute error of test set ($rMAE_{TST}$ - eq. (2)) and were used as performance parameter to stop ANN training repetitions.

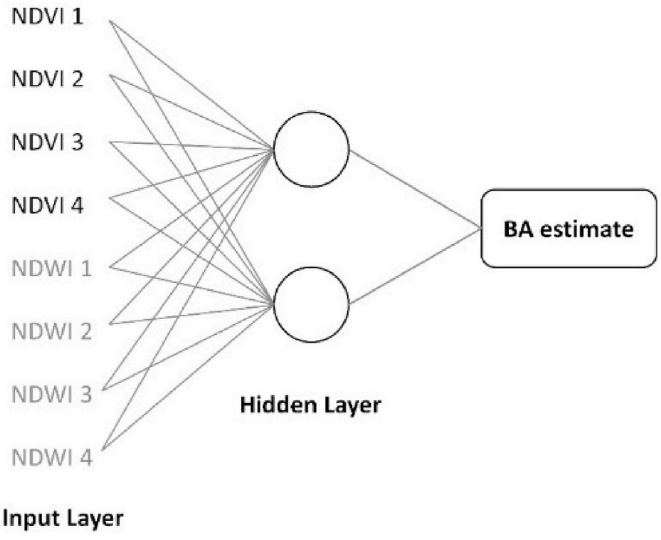

Fig. 3. Final configuration of the trained MLP ANN: 8 inputs and 2 neurons in the hidden layer. This configuration proved to be the best performing one for both confers and broadleaves.

$$rMAE_{TR}(t) = \frac{MAE_{TR}(t)}{\overline{BA}_{TR}} \cdot 100, \cdot rMAE_{TST}(t) = \frac{MAE_{TST}(t)}{\overline{BA}_{TST}} \cdot 100 \quad (2)$$

where $MAE_{TR}(t)$ and $MAE_{TST}(t)$ are the Mean Absolute Error (Willmott and Matsuura, 2005) of BA computed at the generic training *t-th* iteration for the training and test set, respectively; $\overline{BA}_{TST}$ and $\overline{BA}_{TR}$ are the mean BA values for the training and test set, respectively. During training the number of neurons was iteratively changed from 2 up to 6, and, for each ANN design, 10 runs were launched with different random initial weights; the hyperbolic tangent and the linear function were set as transfer functions for the hidden and output layer, respectively and the Levemberg-Marquardt parameter was set to 0.001. After some preliminary tests, authors fixed the following ANN performance thresholds to drive the training: $rMAE_{TR} = 18\%$ and $rMAE_{TST} = 20\%$ for conifers and $rMAE_{TR} = 25\%$ and $rMAE_{TST} = 30\%$ for broadleaves. For both conifers and broadleaves, ANN configuration satisfying the above constraints proved to require 2 neurons and a single hidden layer (Fig. 3).

Once the ANN was successfully trained, a BA map was computed having 40 m resolution for both conifers, $BA^{C}_{(x,y)}$, and broadleaves $BA^{B}_{(x,y)}$.

2.4.2. Forest volume map

Starting from $BA^{C}_{(x,y)}$ and $BA^{B}_{(x,y)}$ and adopting the above-mentioned dendrometric models two maps of V were generated and then mosaicked to obtain as single map of V, $V_{(x,y)}$, to be used by forest managers in planning future actions. A preliminary qualitative evaluation made by forest managers of CFAVS highlighted some criticalities in $V_{(x,y)}$ especially in steepest areas or in anomalous forest stations where specific availability of ecological resources (e.g. light, water, soil, fertility) strongly affect V. Therefore, some correcting factors was estimated and mapped in order to improve V estimates.

Slope Correcting Factor. The errors induced by steep areas were probably related to the satellite acquisition geometry that, recording the projection of the slope onto the horizontal, if not properly compensate for using an accurate DTM, induces an overestimation of V. To refine estimate, $V_{(x,y)}$ was therefore corrected with the slope correcting factor (SCF) calculated according to (eq. (3)) where that slope value ($S_{(x,y)}$ - in radians) was computed from the LiDAR-retrieved DTM.

$$SCF_{(x,y)} = \cos\left(S_{(x,y)}\right) \quad (3)$$

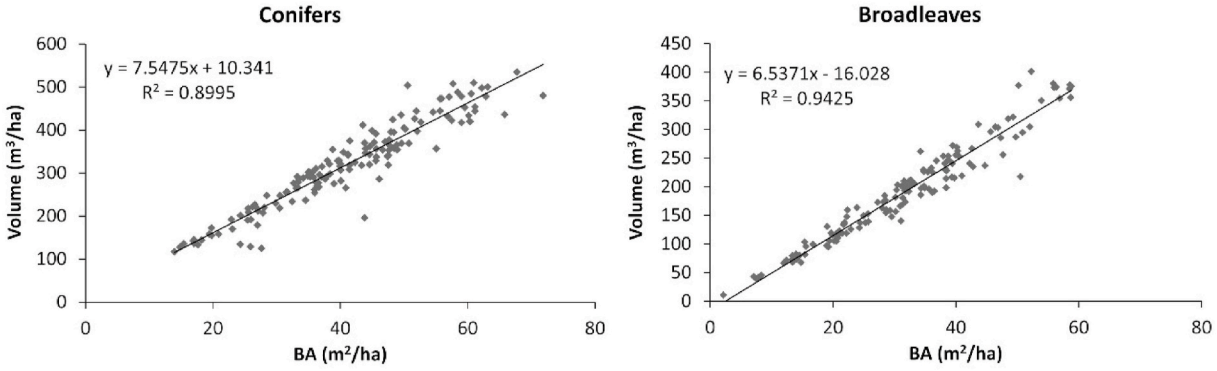

Fig. 4. Scatterplots and regressions (1st order polynomial) relating BA and V. Graphs are given separately for conifers and broadleaves and were obtained from ground measures.

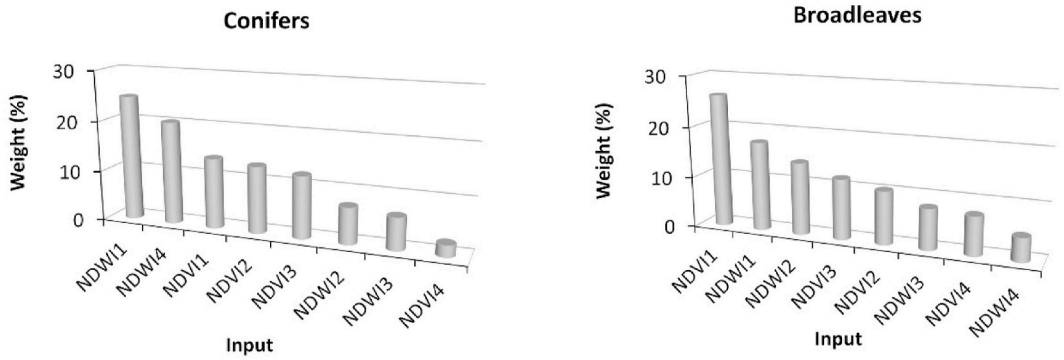

Fig. 5. Relative weights of predictors as resulting from the trained MLP ANN for conifers (left) and broadleaves (right).

Forest Height Correcting Factor. $V_{(x,y)}$ estimate was generated with no regards about the different levels of local fertility in the different stands. Consequently, another correction was applied to refine $V_{(x,y)}$ taking care of this issue, too. A grid difference between DSM and DTM were computed in order to retrieve the canopy height model ($CHM_{(x,y)}$) mapping local tree high. Finally, $CHM_{(x,y)}$ was resampled at the same resolution of $V_{(x,y)}$ (i.e. 40m) and a map of height anomalies, $ha_{(x,y)}$, was generated according to eq. (4).

$$ha_{(x,y)} = \frac{CHM_{(x,y)}}{\mu_{CHM}} \tag{4}$$

Where $CHM_{(x,y)}$ is the local tree height value, μ_{CHM} is the tree height mean value of the considered forest class (conifers and broadleaves) mapped according to forest map of the study area. The final V refined map, $V^{ref}_{(x,y)}$, was obtained by equation (5).

$$V^{ref}_{(x,y)} = ha_{(x,y)} \cdot SCF_{(x,y)} \cdot V_{(x,y)} \tag{5}$$

2.4.3. Validation

Absolute frequency distributions of $V^{ref}_{(x,y)}$ in the private forests for both conifers and broadleaves were computed. Moreover, a comparison between $V^{ref}_{(x,y)}$ and $V_{(x,y)}$ was performed by grid difference ($V^{ref}_{(x,y)} - V_{(x,y)}$) aiming at assessing the improvements induced by correcting factors application (hereafter called ΔV). Finally, the relative MAE (rMAE) was computed using the test set in order to quantify the uncertainty of BA and V estimates.

3. Results

3.1. Dendrometric models

Two dendrometric models were calibrated involving ground data. In particular, BA and V (independent and dependent variable respectively) for conifers and broadleaf trees were separately considered. The regression parameters and defined models were reported in Fig. 4.

The determination coefficient for conifers was about 0.9 while 0.94 for broadleaves highlighting the well fitting between BA and V. These models were subsequently adopted using ANN-retrieved BA as independent variable and V as dependent one.

3.2. ANN-retrieved basal area

Two MLP ANNs were trained separately to generate estimate of BA using the NDVI and NDWI average values from plots computed for the 4 selected images for a total of 8 as ANNs inputs. Fig. 5 shows the relative weights of each input used to design the ANN. It can be noted that: a) for conifers, NDWI seems more affects BA estimates than NDVI and, specifically, the observations at the beginning (June) and end (September) of the growing season are crucial; b) for broadleaves, NDVI and NDWI values at the starting of season seem to be more important in respect of the other acquisitions; conversely, values recorded at the end of season seem to be more negligible.

Successively, trained ANNs were used to generate 2 BA maps for both conifers ($BA^{C}_{(x,y)}$) and broadleaves ($BA^{B}_{(x,y)}$) over the whole area.

3.3. Forest volume map accuracy

To translate BA estimates into the correspondent V one, dendrometric models were applied resulting into new maps ($V^{C}_{(x,y)}$ and $V^{B}_{(x,y)}$). $BA^{C}_{(x,y)}$, $BA^{B}_{(x,y)}$, $V^{C}_{(x,y)}$, $V^{B}_{(x,y)}$, that were finally mosaicked (Fig. 6a and b respectively) to generate a single map of $BA_{(x,y)}$ and $V_{(x,y)}$ having GSD equal to 40 m.

According to eq. (5), $V_{(x,y)}$ was refined to take care about local slope value and local fertility (Fig. 7a and b).

The map of refined volume, $V^{ref}_{(x,y)}$ (Fig. 8a), ΔV map (Fig. 8b) and its pixels distribution (Fig. 8c) are reported in Fig. 8. It can be highlighted that in general $V_{(x,y)}$ overestimated forest volume, in fact the 80% ΔV pixels ranging from 0 to −120 m^3 ha^{-1}. In particular, this overestimation is located in the endalpic and mesalpic parts of the valley (South-Western part of the study area) where many conifers are present (Fig. 1). While the esalpic zone of the valley (North-Eastern part of study area) has ΔV values ranging from ranging from 0 to 70 m^3 ha^{-1}. This zone is mainly characterized by the presence of broadleaves.

Since ΔV map represent a relative comparison of V estimates pre- and post-application of correcting factors applied to ANN regression, to test the accuracy of proposed method, $BA_{(x,y)}$, $V_{(x,y)}$ and $V^{ref}_{(x,y)}$ mean values were computed at each plot in the test set and finally rMAE was calculated to give an accuracy metric of our deductions. BA rMAE for conifers was found equal to 16.3% while for broadleaves equal to 26.9%, denoting worst $BA_{(x,y)}$ estimates in broadleaves probably due to the lower fit between spectral measures and biomass. For how to concern the V estimates, rMAE before and after correcting factors application was reported in Table 3.

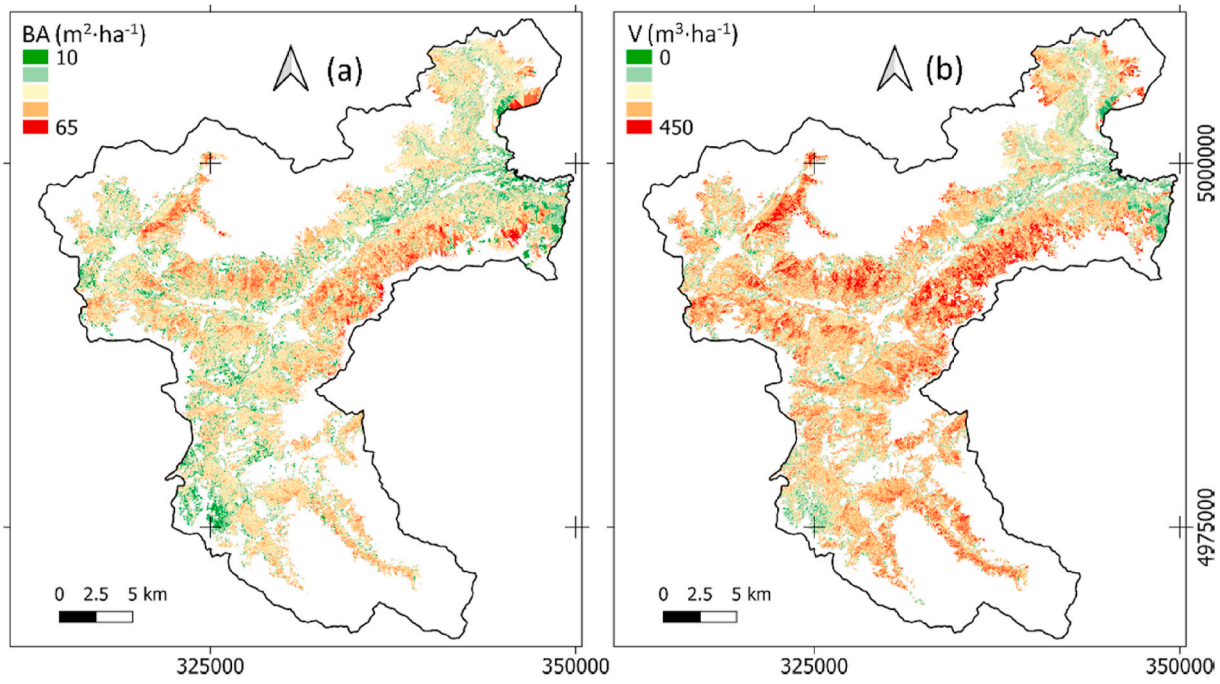

Fig. 6. (a) BA (x,y) map resulted from ANN-based estimation; (b) V (x,y) resulted from dendrometric models' adoption. Reference system is WGS84 UTM 32N.

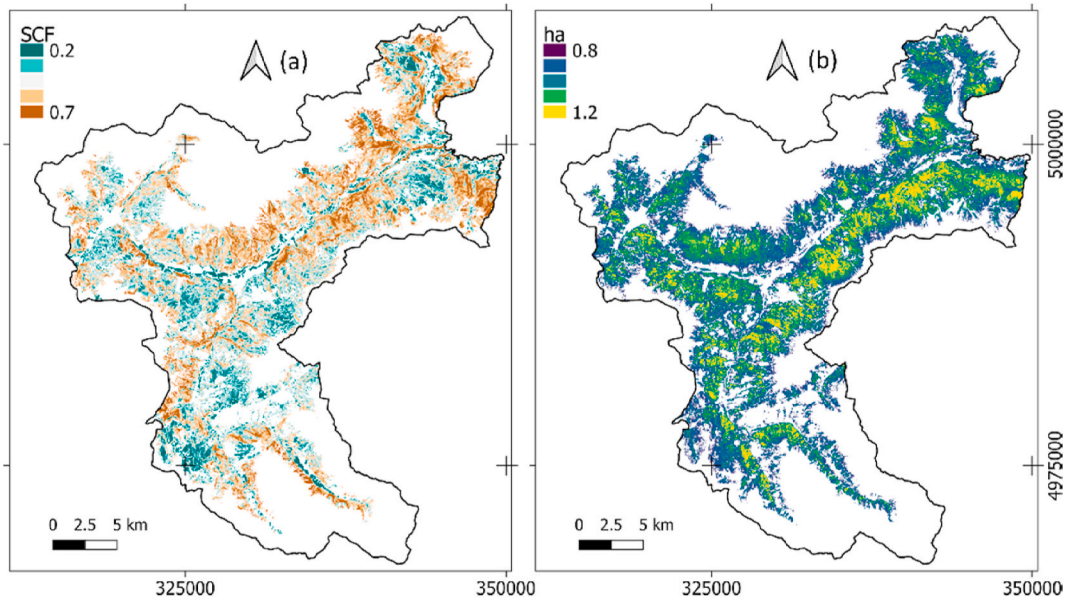

Fig. 7. (a) SCF(x,y) map of slope correcting factor; (b) ha (x,y) map of forest height correcting factor. Reference system is WGS84 UTM 32N.

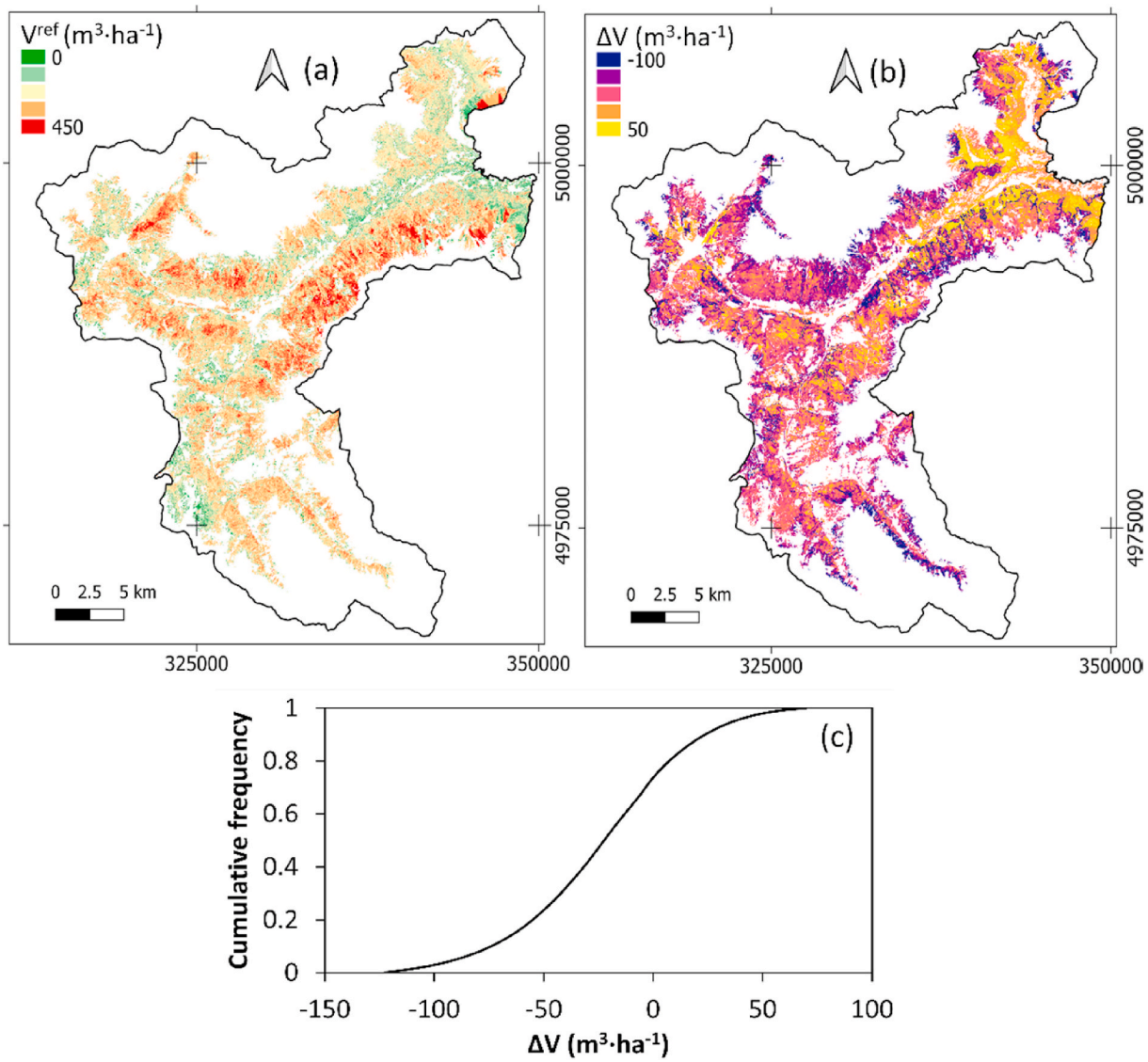

Fig. 8. (a) $V^{ref}_{(x,y)}$ map of refined wood volume; (b) ΔV map; (c) ΔV pixels cumulative frequency distribution. Reference system is WGS84 UTM 32N.

Table 3
rMAE of $BA_{(x,y)}$, $V_{(x,y)}$ and $V^{ref}_{(x,y)}$ estimates involving test set.

	rMAE $\boldsymbol{BA}_{(x,y)}$	rMAE $\boldsymbol{V}_{(x,y)}$	rMAE $\boldsymbol{V}^{ref}_{(x,y)}$
	(%)	(%)	(%)
Conifers	16.29	26.12	24.48
Broadleaves	26.92	62.62	49.29

4. Discussions

It can be highlighted that the adoption of $ha_{(x,y)}$ and $SCF_{(x,y)}$ deeply improved the V estimation, especially for the broadleaves. In fact, rMAE of conifers slightly decreases from 26.12% to 24.48%, otherwise, the broadleaves one had a very high improvement, moving from 62.62% to 49.29%. These results confirm that the incorporation of open auxiliary data, such as LiDAR and topographic information, can significantly improves the estimates obtained by the ANN. Similar results were obtained by Deb et al., (2017) that proved the superiority of ANN in respect of other models in terms of statistical significance and reliability assessment measures for ABG mapping. Moreover, Deb et al. proved that the adoption of LiDAR data was recommended for very high precision modelling in ANN for a wide area study improving ANN estimates.

It is worth to highlight that these accuracies are in general low. Nevertheless, similar results were reported by many authors that adopted Sentinel-2 or Landsat-8 imagery to estimate BA or V denoting an intrinsic limitation of multispectral data adoption for forest biomass estimation (TSITSI 2016; H Nguyen et al., 2020; Laurin et al., 2018; Boyd and Danson 2005). For example: Ahmadi et al., (2020) found a RMSE% 10% concerning BA estimation. Moreover, for how to concern V, Chrysafisa et al. (Chrysafis et al., 2019) found a RMSE% ranging from 30% to 50% according to the Sentinel-2 acquisition period over Greece alps. In spite of these errors, remote sensing-based regression models remain the only reliable and available tools to estimate and map wood volume over wide areas especially while working with private stands where their low economic values do not allow active silvicultural management. Finally, some statistics concerning the distribution of final volume $V^{ref}_{(x,y)}$) in the area were reported in Fig. 9 for both conifers and broadleaves stands.

In the analysed private forests, conifers volume appears to be more homogeneous, while broadleaves one clearly shows a bi-modal behaviour suggesting that two significantly different groups of trees are populating the area. In particular, this broadleaves volume distribution is probably linked to a peculiar phenomenon of the Italian mountain

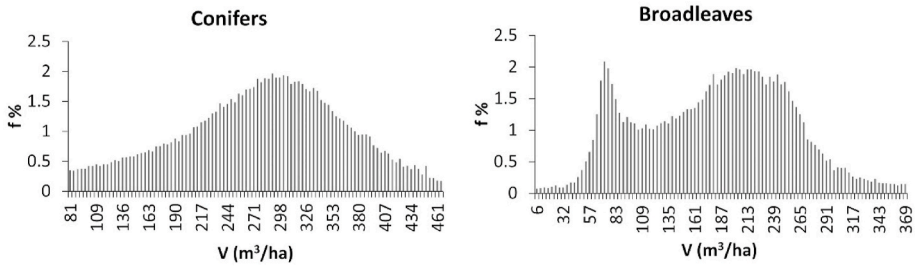

Fig. 9. (left) relative frequency distribution of $V^{ref}_{(x,y)}$ over conifer stands; (right) relative frequency distribution of $V^{ref}_{(x,y)}$ over broadleaves stands in private forests of Susa valley.

region, especially related to private forests. In fact, there are several agricultural areas that were been historically cultivated and during the last decades abandoned which were colonized by woods (i.e. maples and ash) due to a management absence (Minotta and Degioanni 2011). Specifically, these relatively young forests could be related to the first peak in the broadleaves volume distribution while second peak could be related to older stands. Differently, conifers stands are more homogeneous and also their management is not significantly changed in last years. These results show that S2 and open data can effectively support the wood volume mapping in private forest. In fact, traditional field measurements, based on sampling plots, are certainly accurate, but time-consuming and expensive, additionally, such an approach cannot provide a wall-to-wall estimate of measures over large areas. Otherwise, the proposed method, based on model calibration involving few ground data and satellite observations can certainly reduce costs compared to in-depth field surveys, which, intuitively, would require many field surveys (Fassnacht et al., 2014). Especially, while working with private forests, these characteristics allows the constitution of a rough tool giving an estimation of potential economic value of private forests that ordinary is not deeply explored.

5. Conclusions

In this work a methodology for estimation of BA and wood volume of private forest stands over wide areas located in mountain regions was proposed. Results were expected to support forest management by technicians of the High Susa Valley Forest Consortium decreasing ground survey-related costs, thus enhancing the final economic values of private stands.

The proposed methodology relies on freely available satellite imagery from the Copernicus Sentinel-2 mission and low-density LiDAR data; processing is based on Multi-layer Perceptron artificial neural network trained and validated with respect to ground data. Results show that BA estimation has accuracies (rMAE) lower than 28% that are consistent with those expected from the forest sector purposes. It was proved that accuracy of BA estimates is significantly different for conifers (about 16%) and broadleaves (about 26%). V was obtained by 1st order polynomial regression from BA estimates and successively refined taking into account local stands height (deduced from LiDAR data) and mountain slope steepness. Final uncertainty (rMAE) of V estimates resulted 24% for conifers and 49% for broadleaves. With reference to these values a map of BA, $BA_{(x,y)}$, and V, $V^{ref}_{(x,y)}$, were generated to be used in future forest planning by CFAVS technicians with the aim of locating forest stands characterized by higher level of wood biomass and that could be potentially harvested. The methodology proved to reduce field work and therefore the related costs. Moreover, for the first time an estimate of BA and V is given for those areas that usually are not managed, such as the private properties that could be deeply enhanced by such tools.

Funding

This work was supported by EU Rural Development Program - PSR 2014–2020, Regione Piemonte, Operazione 16.1.1, Azione 1 Bando 2016 FEASR - Fondo europeo agricolo per lo sviluppo rurale. Project title: FiLeProPri - Filiera del Legno su Proprietà Privata in Alta Valle di Susa (Wood Production Chain in Private Property Forests in Susa Valley (NW Italy). CUP: J31B16000740009.

Author statement

Evelyn Joan Momo: Conceptualization, Methodology, Software, Data Curation, Writing - Original Draft, Visualization Samuele De Petris: Data curation, Writing- Original draft preparation, Writing - Review & Editing, Validation. Filippo Sarvia: Data Curation, Writing- Original draft preparation, Writing - Review & Editing. Enrico Borgogno-Mondino: Visualization, Methodology, Supervision, Writing- Original draft preparation, Writing - Review & Editing, Funding acquisition, Project administration.

Ethical statement

All ethical practices have been followed in relation to the development, writing, and publication of this article.

Declaration of competing interest

The authors declare that they have no known competing financial interests or personal relationships that could have appeared to influence the work reported in this paper.

Acknowledgements

We would like to thank Dr. Alberto Dotta and Dr. Roberta Berretti for providing ground data and precious local information useful to reach the results presented in this work.

References

Ahmadi, Kourosh, Kalantar, Bahareh, Saeidi, Vahideh, Harandi, Elaheh KG., Janizadeh, Saeid, Ueda, Naonori, 2020. Comparison of machine learning methods for mapping the stand characteristics of temperate forests using multi-spectral sentinel-2 data. Multidisciplinary Digital Publishing Institute Rem. Sens. 12 (18), 3019.

Astola, Heikki, Tuomas, Häme, Sirro, Laura, Molinier, Matthieu, Kilpi, Jorma, 2019. Comparison of sentinel-2 and Landsat 8 imagery for forest variable prediction in boreal region. March Rem. Sens. Environ. 223, 257–273. https://doi.org/10.1016/j.rse.2019.01.019.

Barbachea, Amina, Beghami, Yassine, Benmessaoudc, Hassen, 2018. Study and diachronic analysis of forest cover changes of belezma-Algeria. Geographica Pannonica 22 (4), 253–263. https://doi.org/10.5937/gp22-18806.

Borgogno Mondino, E., Giardino, M., Perotti, L., 2009. A neural network method for analysis of hyperspectral imagery with application to the cassas landslide (Susa valley, NW-Italy). Geomorphology 110 (1–2), 20–27. https://doi.org/10.1016/j.geomorph.2008.12.023.

Borgogno Mondino, E., Fissore, V., Lessio, A., Motta, R., 2016. Are the new gridded DSM/DTMs of the Piemonte region (Italy) proper for forestry? A fast and simple approach for a posteriori metric assessment. iFor. Biogeosci. For. 9 (6), 901–909. https://doi.org/10.3832/ifor1992-009.

Boyd, D.S., Danson, F.M., 2005. Satellite remote sensing of forest resources: three decades of research development. Sage Publications Sage CA: Thousand Oaks, CA Prog. Phys. Geogr. 29 (1), 1–26.

Bravo, Felipe, LeMay, Valerie, Jandl, Robert, von Gadow, Klaus, 2008. Managing Forest Ecosystems: the Challenge of Climate Change. Springer.

Camerano, Paolo, Giannetti, Fabio, Terzuolo, Pier Giorgio, Guiot, Elisa, 2017. La Carta Forestale del Piemonte–Aggiornamento 2016. IPLA SpA–Regione Piemonte. http://www.regione.piemonte.it/foreste/images/files/dwd/Report_Carta_forestale_2016.pdf. (Accessed 7 June 2021).

Chave, Jérôme, Réjou-Méchain, Maxime, Búrquez, Alberto, Chidumayo, Emmanuel, Colgan, Matthew S., Delitti, Welington B.C., Duque, Alvaro, et al., 2014. Improved allometric models to estimate the aboveground biomass of tropical trees. Global Change Biol. 20 (10), 3177–3190. https://doi.org/10.1111/gcb.12629.

Chrysafis, Irene, Mallinis, Giorgos, Siachalou, Sofia, Patias, Petros, 2017. Assessing the relationships between growing stock volume and sentinel-2 imagery in a mediterranean forest ecosystem. Remote Sensing Letters 8 (6), 508–517. https://doi.org/10.1080/2150704X.2017.1295479.

Chrysafis, Irene, Mallinis, Giorgos, Tsakiri, Maria, Patias, Petros, 2019. Evaluation of single-date and multi-seasonal spatial and spectral information of sentinel-2 imagery to assess growing stock volume of a mediterranean forest. Elsevier Int. J. Appl. Earth Obs. Geoinf. 77, 1–14.

Conrad, Olaf, Benjamin Bechtel, Bock, Michael, Dietrich, Helge, Fischer, Elke, Gerlitz, Lars, Jan, Wehberg, Wichmann, Volker, Böhner, Jürgen, 2015. System for automated geoscientific analyses (SAGA) v. 2.1. 4. Geosci. Model Dev. Discuss. (GMDD) 8 (2).

Deb, Dibyendu, Singh, J.P., Deb, Shovik, Datta, Debajit, Ghosh, Arunava, Chaurasia, R.S., 2017. An alternative approach for estimating above ground biomass using resourcesat-2 satellite data and artificial neural network in bundelkhand region of India. Environ. Monit. Assess. 189 (11), 576. https://doi.org/10.1007/s10661-017-6307-6.

Dube, Timothy, Mutanga, Onisimo, Shoko, Cletah, Sam, Adelabu, Bangira, Tsitsi, 2016. Remote sensing of aboveground forest biomass: a Review. May Trop. Ecol. 57, 125–132.

Fang, Lei, Yang, Jian, Zhang, Wenqiu, Zhang, Weidong, Yan, Qiaoling, 2019. Combining allometry and landsat-derived disturbance history to estimate tree biomass in subtropical planted forests. December Rem. Sens. Environ. 235, 111423. https://doi.org/10.1016/j.rse.2019.111423.

Fassnacht, F.E., Hartig, F., Latifi, H., Berger, C., Hernández, J., Corvalán, P., Koch, B., 2014. Importance of sample size, data type and prediction method for remote sensing-based estimations of aboveground forest biomass. Rem. Sens. Environ. 154, 102–114.

Anny Francielly Ataide, Gonçalves, Rodrigues de Moura Fernandes, Márcia, Pereira Martins Silva, Jeferson, Fernandes da Silva, Gilson, Quintão de Almeida, André, Gomes Cordeiro, Natielle, Duarte Caldas da Silva, Lucas, et al., 2019. Wood volume estimation in a semidecidual seasonal forest using MSI and SRTM data. Floresta e Ambiente 26 (1). https://doi.org/10.1590/2179-8087.037918.

Freitas, Simone R., Mello, Marcia CS., Cruz, Carla BM., 2005. Relationships between forest structure and vegetation indices in atlantic rainforest. For. Ecol. Manag. 218 (1–3), 353–362.

Galidaki, Georgia, Zianis, Dimitris, Gitas, Ioannis, Radoglou, Kalliopi, Karathanassi, Vassilia, Tsakiri–Strati, Maria, Woodhouse, Iain, Mallinis, Giorgos, 2017. Vegetation biomass estimation with remote sensing: focus on forest and other wooded land over the mediterranean ecosystem. Int. J. Rem. Sens. 38 (7), 1940–1966. https://doi.org/10.1080/01431161.2016.1266113.

Haywood, Andrew, Stone, Christine, Jones, Simon, 2018. The potential of Sentinel satellites for large area aboveground forest biomass mapping. In: IGARSS 2018-2018 IEEE International Geoscience and Remote Sensing Symposium. IEEE, pp. 9030–9033.

Jiménez, Enrique, Vega, José A., Fernández-Alonso, José M., Vega-Nieva, Daniel, Ortiz, Luis, Pablito, M., López-Serrano, Carlos, A., Sánchez, López, 2017. Estimation of aboveground forest biomass in galicia (NW Spain) by the combined use of LiDAR, LANDSAT ETM+ and national forest inventory data. iFor. Biogeosci. For. 10 (3), 590.

Laurin, Gaia Vaglio, Johannes, Balling, Corona, Piermaria, Walter, Mattioli, Papale, Dario, Puletti, Nicola, Rizzo, Maria, Truckenbrodt, John, Urban, Marcel, 2018. Above-ground biomass prediction by sentinel-1 multitemporal data in Central Italy with integration of ALOS2 and sentinel-2 data. International Society for Optics and Photonics J. Appl. Remote Sens. 12 (1), 016008.

Lessio, Federico, Borgogno Mondino, Enrico, Alberto, Alma, 2011. Spatial patterns of scaphoideus titanus (Hemiptera: cicadellidae): a geostatistical and neural network approach. Int. J. Pest Manag. 57 (3), 205–216.

Lu, Dengsheng, 2006. "The potential and challenge of remote sensing-based biomass estimation". Int. J. Rem. Sens. 27 (7), 1297–1328.

Lu, Dengsheng, Chen, Qi, Wang, Guangxing, Liu, Lijuan, Li, Guiying, Moran, Emilio, 2016. A survey of remote sensing-based aboveground biomass estimation methods in forest ecosystems. International Journal of Digital Earth 9 (1), 63–105.

Minotta, Gianfranco, Degioanni, D., 2011. Naturally regenerated English oak (quercus robur L.) stands on abandoned agricultural lands in rilate valley (piedmont region, NW Italy). SISEF-Italian Society of Silviculture and Forest Ecology iFor. Biogeosci. For. 4 (1), 31.

Monserud, Robert A., 2003. Evaluating forest models in a sustainable forest management context. Citeseer Forest Biometry, Modelling and Information Sciences 1 (1), 35–47.

Morin, David, Planelis, Milena, Guyett, Dominique, Viiiard, Ludovic, Dedieu, Gérard, 2018. Estimation of forest parameters combining multisensor high resolution remote sensing data. In: IGARSS 2018-2018 IEEE International Geoscience and Remote Sensing Symposium. IEEE, pp. 8801–8804.

Morin, D., Planells, M., Guyon, D., Villard, L., Mermoz, S., Bouvet, A., Thevenon, H., Dejoux, J.-F., Le Toan, T., Dedieu, G., 2019. Estimation and mapping of forest structure parameters from open access satellite images: development of a generic method with a study case on coniferous plantation. Rem. Sens. 11 (11) https://doi.org/10.3390/rs11111275.

Mura, M., Bottalico, F., Giannetti, F., Bertani, R., Giannini, R., Mancini, M., Orlandini, S., Travaglini, D., Chirici, G., 2018. Exploiting the capabilities of the sentinel-2 Multi spectral instrument for predicting growing stock volume in forest ecosystems. Int. J. Appl. Earth Obs. Geoinf. 66, 126–134. https://doi.org/10.1016/j.jag.2017.11.013.

Naik, Parth, Dalponte, Michele, Bruzzone, Lorenzo, 2021. Prediction of forest aboveground biomass using multitemporal multispectral remote sensing data. MDPI AG Rem. Sens. 13 (1282), 1282. https://doi.org/10.3390/rs13071282.

Nguyen Trung, H., Jones, Simon, Soto-Berelov, Mariela, Haywood, Andrew, Hislop, Samuel, 2020. Landsat time-series for estimating forest aboveground biomass and its dynamics across space and time: a Review. Multidisciplinary Digital Publishing Institute Rem. Sens. 12 (1), 98.

Nocentini, Susanna, 2009. Structure and management of beech (Fagus sylvatica L.) forests in Italy. iFor. Biogeosci. For. 2 (3), 105.

Nosenzo, A., 2008. A double-entry tree volume table for beech (Fagus sylvatica L.) coppices in piedmont. Forest@.

Pandit, Santa, Tsuyuki, Satoshi, Dube, Timothy, 2018. Estimating above-ground biomass in sub-tropical buffer zone community forests, Nepal, using Sentinel 2 data. Rem. Sens. 10 (4), 601.

Peel, Murray C., Finlayson, Brian L., McMahon, Thomas A., 2007. Updated world map of the Köppen-Geiger climate classification. Hydrol. Earth Syst. Sci. 11 (5), 1633–1644.

Reis, dos, Aparecida, Aliny, Canaan Carvalho, Mônica, Marcio de Mello, José, Gomide, Lucas Rezende, Antônio Carlos Ferraz Filho, Weimar Acerbi Junior, Fausto, 2018. Spatial prediction of basal area and volume in Eucalyptus stands using Landsat TM data: an assessment of prediction methods. N. Z. J. For. Sci. 48 (1), 1. https://doi.org/10.1186/s40490-017-0108-0.

Rizzo, Maria, Gasparini, Patrizia, Tonolli, Sergio, Zoanetti, Roberto, Buffoni, Dino, Dellagiacoma, Francesco, 2019. "Characterizing small private forests and forest owners' motivations and attitudes in Trentino (Eastern Alps, Italy)". Small-scale Forestry 18 (4), 393–410.

Rouse Jr., J. W., Haas, R.H., Schell, J.A., Deering, D.W., 1974. Monitoring Vegetation Systems in the Great Plains with ERTS.

Rumelhart, David E., Hinton, Geoffrey E., Williams, Ronald J., 1985. Learning Internal Representations by Error Propagation. California Univ San Diego La Jolla Inst for Cognitive Science.

Shang, Chen, Paul, Treitz, Caspersen, John, Jones, Trevor, 2019. Estimation of forest structural and compositional variables using ALS data and multi-seasonal satellite imagery. June Int. J. Appl. Earth Obs. Geoinf. 78, 360–371. https://doi.org/10.1016/j.jag.2018.10.002.

Tsitsi, Bangira, 2016. Remote sensing of aboveground forest biomass: a Review. Trop. Ecol. 57 (2), 125–132.

Vacchiano, Giorgio, Berretti, Roberta, Motta, Renzo, Borgogno Mondino, Enrico, 2018. Assessing the Availability of Forest Biomass for Bioenergy by Publicly Available Satellite Imagery.

Willmott, Cort J., Matsuura, Kenji, 2005. Advantages of the mean absolute error (MAE) over the root mean square error (RMSE) in assessing average model performance. Clim. Res. 30 (1), 79–82.

Wittke, Samantha, Yu, Xiaowei, Karjalainen, Mika, Hyyppä, Juha, Puttonen, Eetu, 2019. Comparison of two-dimensional multitemporal sentinel-2 data with three-dimensional remote sensing data sources for forest inventory parameter estimation over a boreal forest. Int. J. Appl. Earth Obs. Geoinf. 76, 167–178.

Xu, Hanqiu, 2006. Modification of normalised difference water index (NDWI) to enhance open water features in remotely sensed imagery. Int. J. Rem. Sens. 27 (14), 3025–3033.

Zhao, Panpan, Lu, Dengsheng, Wang, Guangxing, Wu, Chuping, Huang, Yujie, Yu, Shuquan, 2016. Examining spectral reflectance saturation in Landsat imagery and corresponding solutions to improve forest aboveground biomass estimation. Rem. Sens. 8 (6), 469.